CANCER GENOMICS & PROTEOMICS *1*: 231-240 (2004)

Increased Expression of the Genes for Mitotic Spindle Assembly and Chromosome Segregation in Both Lung and Pancreatic Carcinomas

KENJI HAMADA[1], MICHIO UEDA[3], MASAMI SATOH[2], NAOHITO INAGAKI[1], HIROSHI SHIMADA[3] and HISAFUMI YAMADA-OKABE[1]

[1]Pharmaceutical Research Department IV, Kamakura Research Laboratories, Chugai Pharmaceutical Co. Ltd., 200 Kajiwara, Kamakura, Kanagawa 247-8530; [2]Department of Surgery, Tohoku University, 4-1 Seiryoucho, Aobaku, Sendai, Miyagi 980-8575; [3]Department of Surgery, School of Medicine, Yokohama City University, 3-9 Fukuura, Kanazawa, Yokohama, Kanagawa 236-0004, Japan

Abstract. *Genes whose expression was modulated in two different tumor types, lung or pancreatic carcinoma, were identified by DNA microarray and subsequent expression correlation analyses. For more accurate comparison of the gene expression between tumor and normal cells, tumor cells and normal epithelium cells were isolated by laser-captured microdissection. Genes whose expression was significantly altered in lung carcinomas or pancreatic carcinomas as compared to their normal counterparts were ranked by the T-values calculated from the Fisher's ratios and their corresponding background Fisher's ratios, followed by statistical confirmation using the Welch's t-test. Among the genes that were ranked in the top 150, either in lung carcinomas or pancreatic carcinomas, expressions of MAD2, BUB1, BUB1B, HEC, CENPE, ZWINT, KNSL1, SMC4, CCNB, TK and PMS2L6 were found to be significantly up-regulated in both tumor types. Interestingly, 8 of the above 11 genes code for the proteins involved in the mitotic spindle assembly and chromosome segregation. Furthermore, the search for genes whose expression correlated with one of the above 5 genes yielded additional genes that are also considered to be involved in mitotic spindle assembly and chromosome segregation. Thus, increased expression of the genes for mitotic spindle assembly and chromosome segregation are a common feature of at least lung carcinomas and pancreatic carcinomas and, therefore, such genes may be potential targets for widely effective anticancer agents.*

Correspondence to: Hisafumi Yamada-Okabe, Pharmaceutical Research Department IV, Kamakura Research Laboratories, Chugai Pharmaceutical Co. Ltd., 200 Kajiwara, Kamakura, Kanagawa 247-8530, Japan.

Key Words: Non-small cell lung carcinomas, pancreatic adenocarcinomas, DNA microarray, laser-captured microdissection, gene expression, mitotic spindle assembly, chromosome segregation, spindle checkpoint.

Lung cancer and pancreatic cancer are among the most frequent causes of cancer death worldwide. Although new molecular-targeting drugs such as Iressa and Gemzar have been introduced into their treatment, the efficacy of chemotherapeutic agents against these cancers is still limited (1, 2). Since lung and pancreatic cancers are often asymptomatic in their early stages, most patients have widespread disease at the time of diagnosis. Genome-wide gene expression analysis by DNA microarray with surgical specimens has led to the identification of new sets of genes involved in the development and growth of tumors, metastasis, prognosis and sensitivity and resistance to drugs in many cancer types (3, 4).

DNA microarray is a powerful technique for comprehensive analysis of gene expression, though a method for extracting genes of interest from a large number of genes using a relatively small number of samples has not been well established. Previously, we adopted a combination of the Fisher's ratio and the leave-one-out method to analyze DNA microarray data and identified genes that were differentially expressed between HBV- and HCV-infected hepatocellular carcinomas (5, 6).

In an attempt to understand more about the fundamental molecular characteristics of lung and pancreatic cancers and to identify useful molecules for therapies and diagnosis across different tissue and tumor types, we analyzed the gene expression profiles of two different tumor types, lung carcinomas and pancreatic carcinomas, and compared the results with profiles of their normal counterparts.

Because of a higher percentage of stromal cells such as fibroblasts within lung and pancreatic tumor tissues, gene

expression profiling of these tumor tissues is rather complicated. To achieve an accurate comparison of the gene expression profiles of tumor and normal cells, cells in tumor tissues and their normal counterparts, *i.e.* normal epithelia of lung and pancreatic ducts, were isolated by laser-captured microdissection. For DNA microarray data analysis, T-values from Fisher's ratio and its corresponding background Fisher's ratio were applied to select genes whose expression was significantly altered in tumor tissues; the significance of the expression was statistically confirmed by Welch's *t*-test. By this gene selection procedure, we found that the expression of the 8 genes that are involved in spindle checkpoint and function during the metaphase to anaphase transition are up-regulated in both lung carcinomas and pancreatic carcinomas. Furthermore, a search for genes whose expression correlated with that of these 8 genes yielded additional genes responsible for mitotic spindle assembly and/or chromosome segregation. Thus, the altered expression of the genes for the metaphase to anaphase transition seems a common and important cellular response in tumor cells *in vivo*.

Materials and Methods

RNA isolation from microdissection sample. Samples of lung carcinoma and pancreas carcinoma were collected at Tohoku University Hospital and Yokohama City University Hospital, Japan, respectively. Written informed consent was obtained from all patients before surgery and the study protocol was approved by the Institutional Review Board for the Use of Human Subjects at each university. Tumor cells and non-tumorous normal cells were isolated by laser capture microdissection (model LM200, Arcturus, CA, USA). RNA isolation from microdissected samples was done with a Micro RNA Isolation Kit (Stratagene, CA, USA) according to the instruction manual.

cRNA synthesis and hybridization. Biotin-labeled cRNA was synthesized by two rounds of cDNA synthesis. In the first round, cDNA was synthesized from 20-50 ng of total RNA with 5 pmole of T7-promoter-linked (dT)-24 primer, 5'-GGCCAGTGAATTGTAA TACGACTCACTATAGGGAGGCGG-(T)24-3', in RT-buffer containing 0.5 mM dNTPs, 10mM DTT, 5mM $MgCl_2$ and 50 units of SuperScript II Reverse Transcriptase (Invitrogen, CA, USA) at 42˚C for 1 h. Reverse strand cDNA was synthesized at 16˚C for 2 h in a buffer containing 0.2mM dNTPs, 40 units of *E.coli* DNA polymerase, 1 unit of *E.coli* DNA ligase and 2 units of RNase H. Next, T4 DNA polymerase (10 units) was added to the reaction mixture and incubation was continued at 16˚C for 5 min. The resulting cDNA was purified with Phase Lock Gel Light (Eppendorf, Germany), precipitated in ethanol and used as the template for cRNA synthesis. cRNA was synthesized with T7 RNA polymerase (MEGAscript, TX, USA) in a buffer containing 7.5mM of dNTPs at 37˚C for 6 h, purified with RNeasy (QIAGEN, CA, USA), precipitated in ethanol and used as the template for the second round of synthesis. In the second round, cDNA was synthesized in a buffer containing all the cRNA synthesized in the first round, 1 μg of random hexamer (Invitrogen) 0.5 mM dNTPs, 10mM DTT, 5mM $MgCl_2$ and 50 units of SuperScript II RT at 25˚C for 10 min followed by 50-min incubation at 42˚C. RNase H (2 units) was then added to the reaction mixture and incubation was continued at 37˚C for 20 min. After inactivation of RNase H at 95˚C for 2 min, reverse strand cDNA was synthesized with the T7-promoter linked (dT)-24 primer at 16˚C for 2h, purified with Phase Lock Gel Light, separated from the oligo-hexamer by QIAquick (QIAGEN), and precipitated in ethanol. The biotin-labeled cRNA was synthesized from the second round cDNA as a template. The cDNA was incubated in a buffer containing T7 RNA polymerase, 7.5 mM each of ATP, GTP and biotin-CTP, and biotin-UTP at 37˚C for 6 h. The resulting cRNA was purified with RNeasy (QIAGEN) and precipitated in ethanol. This procedure yielded approximately 100 μg of biotin-labeled cRNA from 20-50 ng of total RNA. After confirming the quality of cRNA by electrophoresis, 30 μg of the cRNA was fragmented in a buffer containing 40 mM Tris-acetate, pH 8.1, 100mM KOAc and 30 mM MgOAc at 95˚C for 35 min.

Ten micrograms of the fragmented cRNA were used for the hybridization with Affymetrix GeneChip®. Hybridization, washing, staining, amplification of the signals and scanning of the signals were carried out as described in previously (5, 6). The signal was calculated and normalized (global scaling by target intensity at 300) with Affymetrix Microarray Suite software (ver. 4.0).

Statistical analysis and selection using Fisher's ratio. Gene selection was carried out using a two-step selection procedure. Genes whose expression was significantly different between the two groups were selected according to the T-value calculated by Fisher's ratio and background Fisher's ratio (5,6), followed by statistical confirmation from Welch's *t*-test.

The Fisher's ratio for the jth gene was calculated by the formula:

$$F(j)=(\mu j(A)-\mu j(B))2/(P(A)\sigma\text{–}j^2(A)+P(B)\sigma\text{–}j^2(B))$$

where μj represents the mean value, $\sigma\text{–}j^2$ represents the variance, and P represents the number of the *a priori* probability. To reduce sampling error, Fisher's ratio was calculated for all $[{}_{nA}C_{nA-1} \times {}_{nB}C_{nB-1}]$ sample combinations generated by extracting one sample from each group (A and B); distributions of all sample combinations were determined.

Distribution was evaluated using the background Fisher's ratio that was calculated from randomly generated sample combinations, where samples were randomly divided into two groups consisting of n_A and n_B irrespective of their cell types, *i.e.*, tumor or normal cells. In this process, the random permutation method was applied 1000 times to produce a background distribution.

Distribution of the Fisher's ratios is symmetrical for the average values when two groups are different, whereas the average of the Fisher's ratio is close to 0 and the distribution takes positive value if two groups are not different. Therefore, the Fisher's ratio's distribution generated by 1000 random trials was adjusted by the distribution of a presumptive 2000 trials that was symmetrical to the Y axis, where the average Fisher's ratio is 0. Then, each gene was ranked according to a T-value for z-test between distributions of the true Fisher's ratio and background Fisher's. The T-value for the *j*th gene was calculated by following formula:

$$T_j=(F_{j\ avg.\ of\ true}-F_{j\ avg.\ of\ bg})\ /\ (\sigma\text{–}_j{}^{F}{}_{true}{}^{2}/n_{true}+\sigma\text{–}_j{}^{F}{}_{bg}{}^{2}/n_{bg})^{0.5}$$

where $F_{j\ avg.\ of\ true}$, $F_{j\ avg.\ of\ bg}$, $\sigma\text{–}_j{}^{F}{}_{true}{}^{2}$, n_{true}, $\sigma\text{–}_j{}^{F}{}_{bg}{}^{2}$ and n_{bg} are the mean of Fisher's ratio, the mean background Fisher's ratio,

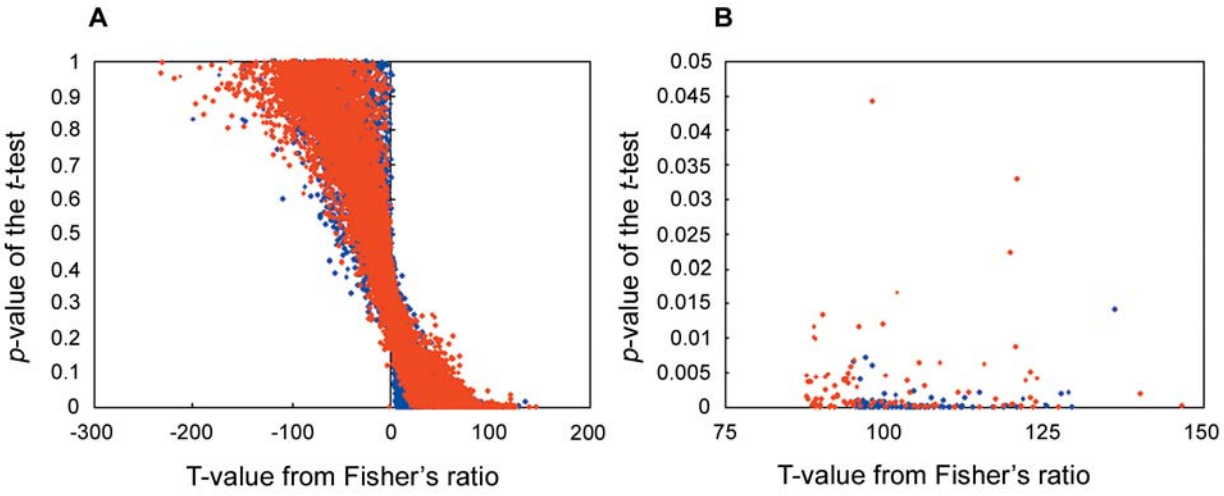

Figure 1. *T-values calculated from Fisher's ratio and p-values from Welch's t-test. T-values for each gene were calculated from Fisher's ratio and background Fisher's ratio and plotted along with p-values of Welch's t-test. A: Double plot of the T-values and p-values for all genes. B: Double plot of the T-values and p-values for the top 150 genes selected according to the T-values. Blue dots and red dots indicate genes selected from lung tissues and from pancreas tissues, respectively. All the top 150 genes selected by T-value show statistical significance ($p<0.05$) as shown in panel B.*

variance of true Fisher's ratio, the number of sample sets for calculating true Fisher's ratios, variance of background Fisher's ratios and the number of sample sets for calculating background Fisher's ratios. In addition, $\sigma_{-j}^{F}{}_{bg}$ was replaced by $(1000\text{-}1/2000\text{-}1)^{0.5}$ x $\sigma^{F}{}_{bg}$ for correction. The absolute value of T-values were not considered because $F_{j\ avg.\ of\ true} > F_{j\ avg.\ of\ bg}$ is important in this process. Finally, the significance of differences in the expression of the selected genes was validated by Welch's *t*-test, which is indicated as the *p*-value.

Gene clustering and Pearson's correlation analysis. Clustering was performed with a hierarchical clustering tool (7) after normalizing each gene expression and calculating the average distance. Pearson's correlation was calculated using Microsoft EXCEL. GeneSpring 5.0 (Silicon Genetics, CA, USA) was used for gene ontology classification .

Results

To profile the gene expressions of the two tumor types, laser-capture microdissection was used for the DNA microarray because lung tumor and pancreatic tumor tissues often contain large portions of stroma cells such as fibroblasts. For the comparison of gene expression profiles between tumor cells and corresponding normal tissues, we isolated cells from the normal epithelium of lung and pancreatic ducts. Total RNA was isolated from approximately 2,000 cells of 14 lung carcinomas, 9 normal lung epithelia, 13 pancreatic carcinomas and 13 normal epithelia of pancreatic ducts. Because the total RNA extracted from the dissected cells (20-100 ng) was not sufficient to generate cRNA for hybridization, it was amplified by twice repeating the synthesis of cDNA and cRNA.

To identify the genes whose expression was significantly different between tumor and normal cells, we calculated Fisher's ratios for various combinations of the sample sets. For lung tissues, we created 14 different sample sets consisting of 13 lung carcinomas and 9 different sample sets consisting of 8 normal lung epithelia. The average and standard deviation of the Fisher's ratios between tumor and normal from all 126 (14 x 9) combinations were calculated for each gene. To evaluate the distribution of the true Fisher's ratio, mean background Fisher's ratios were calculated from 1000 randomly-generated sample sets, which were further adjusted by the distribution of 2000 presumptive trials (see Materials and Methods). Then, the true Fisher's ratios for each gene were ranked in order of T-values for the z-test, that was determined with the true and background Fisher's ratios. The same analysis was performed with pancreatic carcinomas and normal epithelium of the pancreatic ducts, and the genes ranked based on the order of the T-values. Figure 1 shows a scattered plot of T-values and *p*-values determined by the Welch's *t*-test in each gene. In both lung carcinomas and pancreatic carcinomas, all of the top 150 genes ranked by this method showed *p*-values less than 0.05 (Figure 1 B).

When the lung tissue specimens were clustered with genes that were ranked in the top 150, tumor and normal samples were clearly separate; the same was also true for pancreatic tissue specimens (Figures 2 and 3). Among the top 150 ranked genes for lung or pancreatic tissues, many encode proteins responsible for the mitotic spindle assembly and/or chromosome segregation that function at G2-M transition. We therefore examined whether the expressions of genes

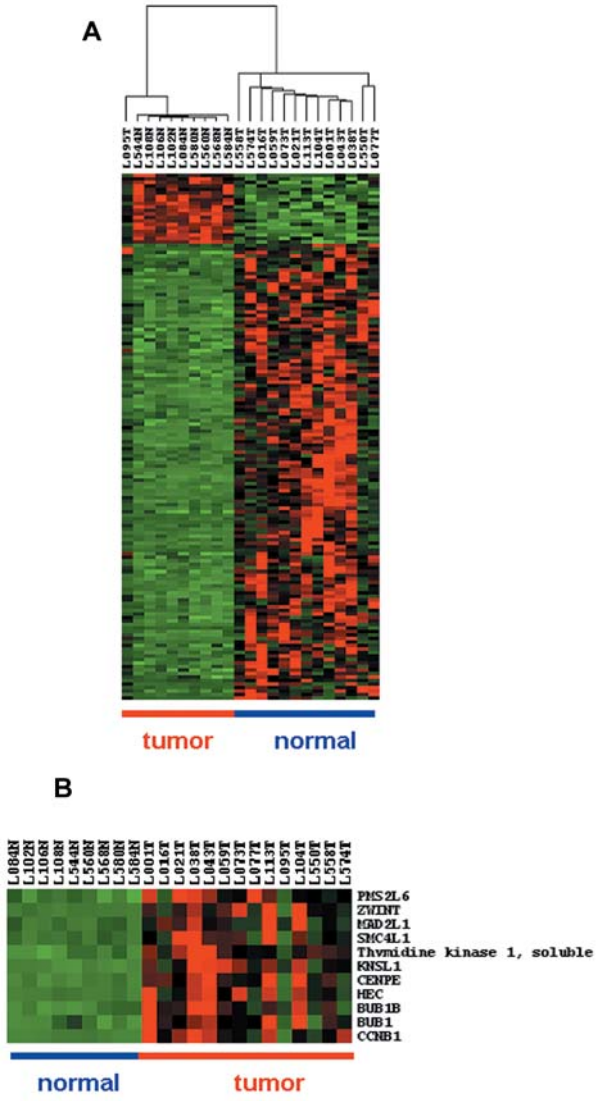

Figure 2. *Separation of tumor cells from normal cells by clustering with genes selected according to T-values in lung tissues. Lung carcinoma tumor and epithelium of normal tissues were clustered with the top 150 genes selected according to their T-values (A) and with the 11 genes that were commonly selected in both lung and pancreas tissues (B). Eight out of the 11 genes that were commonly selected in both lung and pancreas tissues are responsible for spindle and/or kinetochore. Note that the expression of the 8 genes was up-regulated in tumor cells compared with normal cells in lung.*

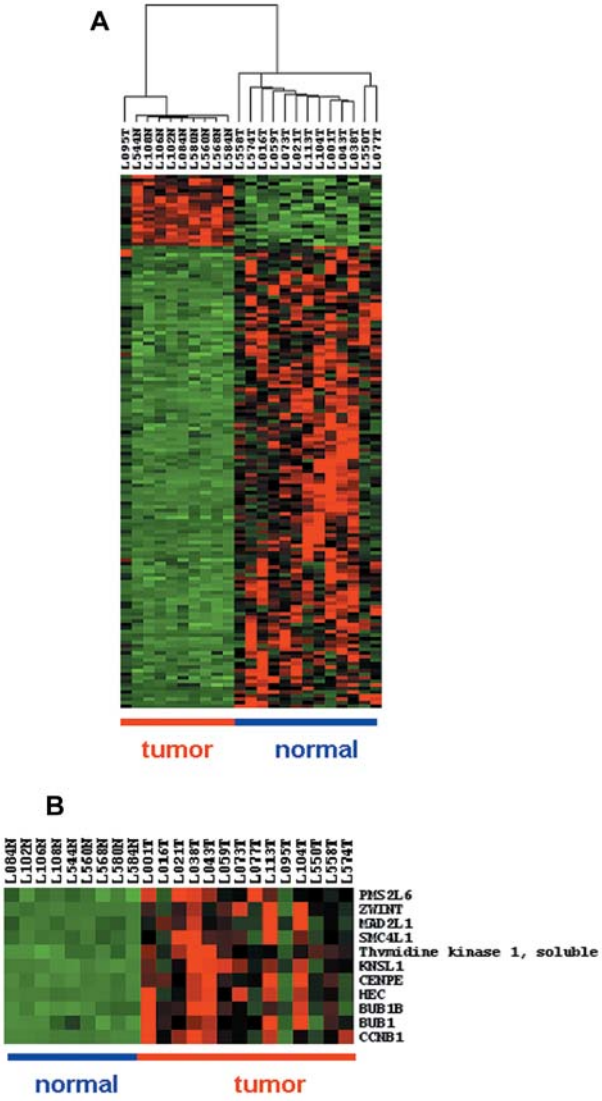

Figure 3. *Separation of tumor cells from normal cells by clustering with genes selected according to their T-values in pancreatic tissues. Pancreatic carcinoma (tumor) and pancreatic duct epithelium (normal) tissues were clustered with the top 150 genes selected according to their T-values (A) and with the 11 genes that were commonly selected in both lung and pancreas tissues (B). Eight out of the 11 genes that were commonly selected in both lung and pancreas tissues are responsible for spindle and/or kinetochore. Note that the expression of the 8 genes was up-regulated in tumor cells compared with normal cells in pancreas.*

involved in the spindle and kinetochore were different between tumor and normal cells in lung and pancreatic tissues. According to the classification of the genes based on annotation using the GeneSpring ontology, the Affymetrix U95A chip appeared to contain 42 probes for the spindle- and kinetochore-related genes. Clustering the lung or pancreatic tissues with the 42 genes also clearly distinguished tumor tissues from normal tissues (Figure 4). These results indicate that one of the most significant differences in the gene expression profiles between tumor and normal tissues is the modulation of the expression of the genes for spindle, kinetochore and their related functions.

In an attempt to identify common changes in gene expression among tumors of different tissue types and stages, we looked for genes whose expression was altered in both lung carcinomas and pancreatic carcinomas. Among the top

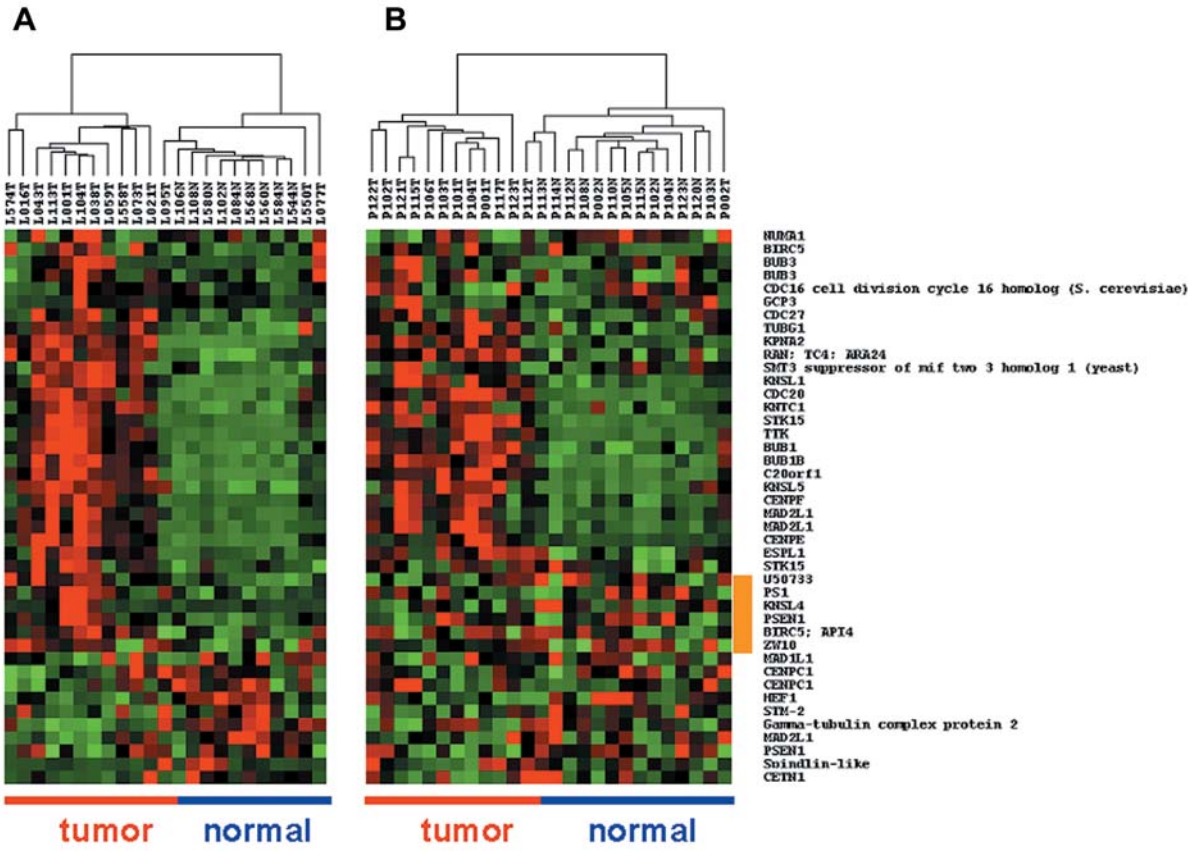

Figure 4. *Separation of tumor cells from normal cells by clustering with genes for kinetochore- and spindle-related genes. Tumor and normal tissues of lung (A) and pancreas (B) were clustered with 42 genes that are classified as kinetochore- and spindle-related genes. Kinetochore- and spindle-related genes in the probes of the Affymetrix GeneChip U95A ver.2 were selected based on the ontology classification of genes by GeneSpring. Expression patterns between tumor and normal cells of most of genes are similar in pancreas and lung, but those of genes with orange bars (U50733, PS1, KNSL4, PSEN1, BIRC5 and ZW10) show different patterns.*

150 ranked genes whose expression was significantly altered in lung carcinomas and pancreatic carcinomas as compared to their normal counterparts, 11 genes were found whose expression was up-regulated in both tumors: *MAD2L1, KNSL1, ZWINT, BUB1B, PMS2L6, CENPE, TK (thymidine kinase), HEC, SMC4L1, CCNB1* and *BUB1* (Figures 2B, 3B and Table I). Although PMS2L6 and TK are responsible for DNA mismatch repair and DNA synthesis, respectively (8, 9), other genes encode proteins for mitotic spindle assembly and/or chromosome segregation. *BUB1* (10), *BUB1B* (11, 12), *CENPE* (13) *HEC* (14) and *MAD2* (15-18) proteins serve as spindle checkpoints by inactivating the *CDC20* protein (19-21). We therefore asked whether the expression of *BUB1, BUB1B, CENPE, HEC,* or *MAD2L1* correlated with that of *CDC20*. As shown in Figure 5, expression of *CDC20* was also up-regulated in tumors compared to normal tissues, but it did not correlate well with the expression of the above 5 genes. However, there was a clear correlation between the expression of *HEC* and that of *BUB1B* in both lung carcinomas and pancreatic carcinomas (Figure 5F). The search for genes whose expression correlated to that of *BUB1, BUB1B, CENPE, HEC,* or *MAD2L1* with a *p*-value less than 0.01, in both lung carcinomas and pancreatic carcinomas, yielded 40 genes. Among these 40 genes, 13 genes turned out to be responsible for the spindle and/or kinetochore, or chromosome segregation-related genes. As shown in Table II, the expression of *BUB1* correlated with that of *HSP90, HEC,* alpha-centractin, *CENPE* and topoisomerase truncated form, and that of HEC correlated with those of *TOPBP1, STK15, YES1* and *CCNB1*. Furthermore, there were clear correlations of the expression between *TTK* and *TOP2A*, between *MAD2L1* with *CENPF*, and between *MAD2L1* and a gene for kinesin-related protein. All of the genes described above encode proteins involved in spindle assembly and/or chromosome segregation at the metaphase to anaphase transition. Together, these

Table I. *Genes that were commonly identified in top 150 selected genes in lung and pancreas tissue samples.*

				lung				panc			
probe set	Common	Genbank	Map	N-average	T-average	T/N=	*p*-value of *t*-test	N-average	T-average	T/N=	*p*-value of *t*-test
37282_at	MAD2L1	AJ000186	4q27	16.7±16.2	150.5±119.5	9.0	0.00106	22.3±10.2	65.8±42.3	2.9	0.00307
40726_at	KNSL1	U37426	10q24.1	31.3±15.2	353.5±183.3	11.3	0.00002	70.4±28.7	192.3±89.1	2.7	0.00032
35995_at	ZWINT	AF067656	10q21-q22	162.2±43.8	1535.6±1018.0	9.5	0.00022	263.0±93.9	770.3±152.1	2.9	0.00000
35699_at	BUB1B	AF053306	15q15	87.6±37.9	407.1±207.3	4.6	0.00006	67.6±17.0	193.6±44.5	2.9	0.00000
32310_f_at	PMS2L6	AI341574	7q11-q22	89.5±31.6	272.0±121.9	3.0	0.00007	105.6±45.4	178.3±45.5	1.7	0.00043
37173_at	CENPE	Z15005	4q24-q25	7.0±3.5	62.1±34.6	8.9	0.00004	6.3±1.7	22.8±22.7	3.6	0.02226
41400_at	Thymidine kinase 1	K02581	16	172.9±62.9	645.0±283.2	3.7	0.00002	223.8±72.3	476.2±189.1	2.1	0.00040
40041_at	HEC	AF017790	18p11.31	91.3±24.6	737.1±457.6	8.1	0.00015	128.1±74.4	368.8±138.6	2.9	0.00003
34878_at	SMC4L1	AB019987	3q26.1	73.6±30.4	389.3±273.6	5.3	0.00083	51.5±22.2	135.4±86.2	2.6	0.00448
34736_at	CCNB1	M25753	5q12	20.8±13.4	399.6±246.3	19.2	0.00007	54.8±24.9	218.3±90.2	4.0	0.00002
41081_at	BUB1	AF053305	2q14	22.5±12.8	95.9±50.9	4.3	0.00011	19.5±9.9	52.7±14.9	2.7	0.00000

T/N: fold change from average.

Table II. *Genes whose expression correlated with that of sprindle checkpoint genes and are annotated as kinotochore, sprindle and/or cell cycle regulator.*

				lung				panc			
				R=		*p*-value		R=		*p*-value	
correlation with	probe set	name	Genbank	normal	tumor	normal	tumor	normal	tumor	normal	tumor
BUB1	33984_at	HSP90	M16660	0.20827	0.66632	0.59076	0.00927	0.27428	0.76149	0.36448	0.00249
BUB1B	40041_at	HEC	AF017790	0.17073	0.80793	0.66053	0.00047	0.32325	0.75760	0.28134	0.00270
BUB1B	40052_at	alpha-centractin	X82206	0.04522	0.66539	0.90803	0.00940	0.17569	0.68711	0.56588	0.00947
CENPE	904_s_at	topisomerase truncated form	L47276	0.35131	0.75735	0.35390	0.00171	0.07661	0.82605	0.80356	0.00050
CENPE	572_at	TTK	M86699	0.26738	0.71506	0.48671	0.00405	0.15075	0.80071	0.62301	0.00101
CENPE	40145_at	TOP2A	AI375913	0.40864	0.71436	0.27484	0.00410	0.11770	0.76879	0.70176	0.00213
HEC	38834_at	TOPBP1	D87448	0.46506	0.85710	0.20716	0.00009	0.27504	0.69860	0.36310	0.00790
HEC	34852_g_at	STK15	AF011468	0.79709	0.82081	0.01010	0.00032	0.50624	0.72144	0.07753	0.00538
HEC	1674_at	YES1	M15990	0.39334	0.68805	0.29495	0.00652	0.05013	0.87856	0.87082	0.00008
HEC	34736_at	CCNB1	M25753	0.28043	0.67576	0.46483	0.00798	0.52419	0.73341	0.06594	0.00433
MAD2L1	1721_g_at	MAD2L1	U65410	0.20799	0.93691	0.59127	0.00000	0.73235	0.80665	0.00442	0.00086
MAD2L1	37302_at	CENPF	U30872	0.51337	0.81226	0.15750	0.00042	0.64759	0.90752	0.01671	0.00002
MAD2L1	38933_at	kinesin related protein	AL021366	0.14247	0.66756	0.71463	0.00909	0.53421	0.77461	0.06003	0.00018

Among 40 that were identified by the expression correlation analysis with spindle checkpoint genes, 13 genes that are annotated as kinetochore, spindle and/or cell cycle regulator are indicated.

results suggest that up-regulation of the expression of the genes for mitotic spindle and chromosome segregation is a common feature of tumor cells in at least lung and pancreatic cancers.

Discussion

We selected 150 genes whose expression was modulated in lung carcinomas or pancreatic carcinomas as compared to their normal counterparts, *i.e.* epithelium of lung and pancreatic ducts. To avoid the stroma cells from gene expression analysis, DNA microarray was performed with tumor cells and corresponding normal cells isolated by laser capture microdissection. Previous reports also compared the gene expression profiles of pancreatic adenocarcinomas with normal epithelium of ducts (22, 23). In this study, we looked for genes that were commonly up-regulated or down-regulated in different tumor types, and gene expression profiling was carried

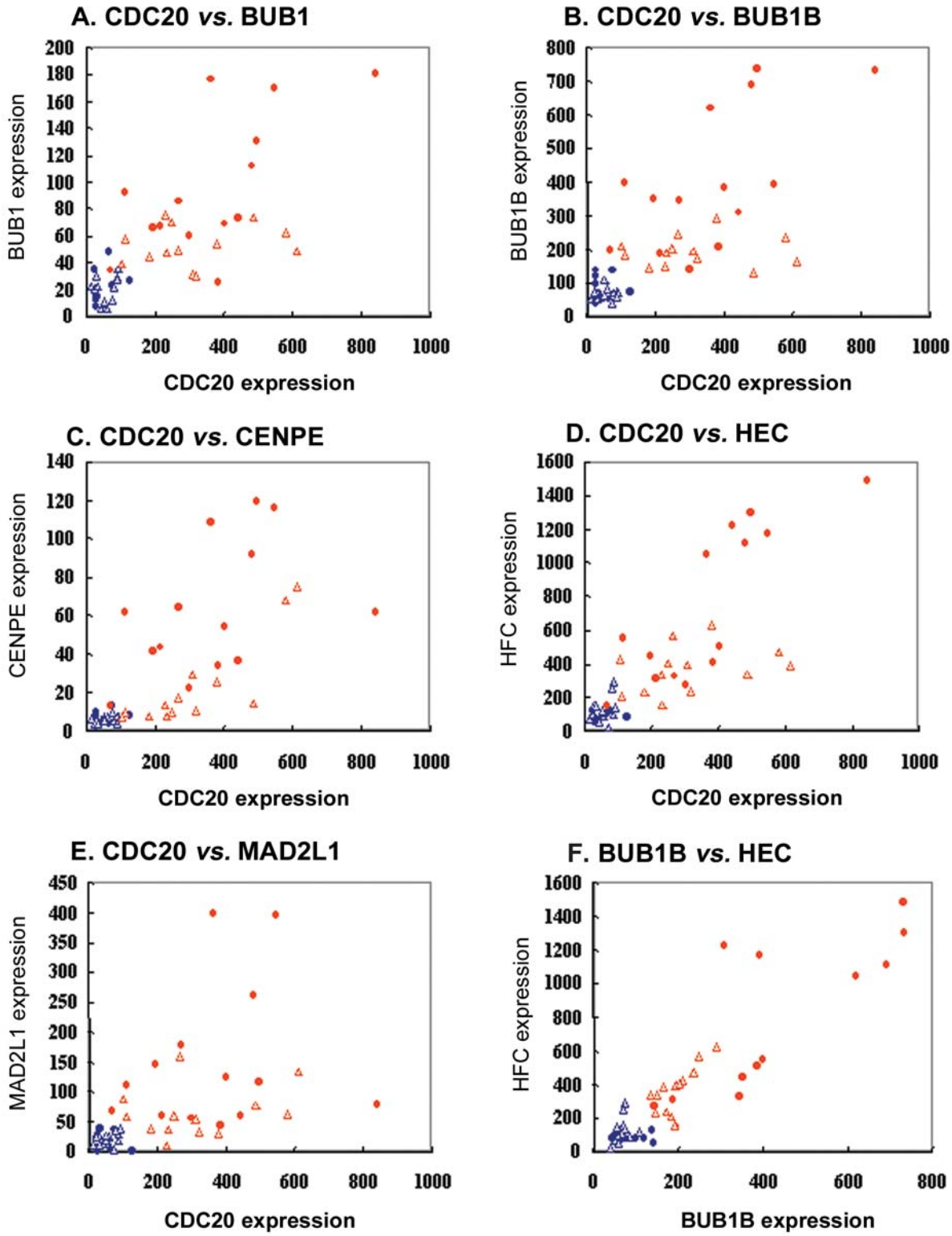

Figure 5. *Correlation of the expressions between CDC20 and spindle checkpoint genes. Correlations of the expression of the CDC20 and spindle checkpoint genes such as BUB1, BUB1B, CENPE, HEC and MAD2L1 were examined. The expression of CDC20 in each sample was plotted with that of BUB1 (A), BUB1B (B), CENPE (C), HEC (D) and MAD2L1 (E). Correlation of the expression between BUB1B and HEC is also indicated (F). Gene expression in tissue is indicated as follows: red circles, lung carcinomas; blue circles, normal lung epithelium; red triangles, pancreatic carcinomas; and blue triangles, epithelium of normal pancreatic ducts. Note that there is a positive correlation between the expression of BUB1B and HEC (F).*

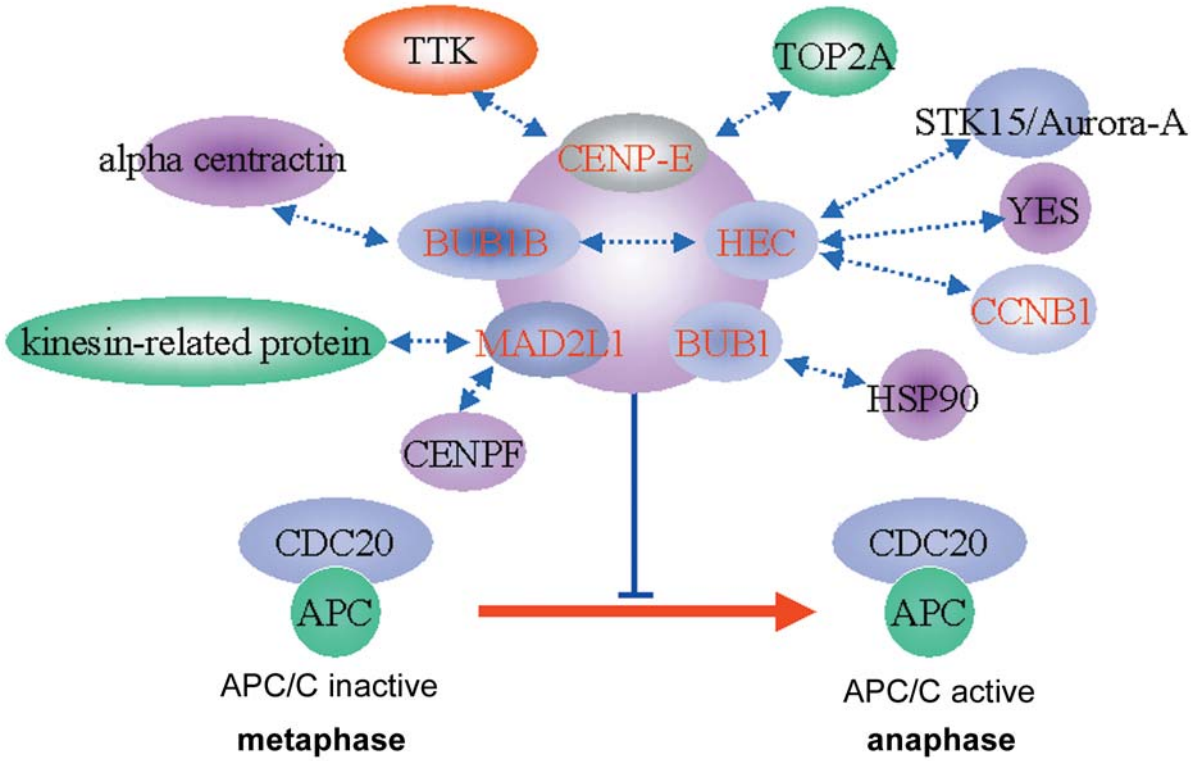

Figure 6. *Predicted expression network of spindle checkpoint genes, cell cycle regulators and kinetochore binding proteins in tumor cells. An expression network of the genes for spindle checkpoint, cell cycle regulation and kinetochore binding was predicted based on the gene expression profile and correlation analysis of the genes that are involved in spindle checkpoint. In lung and pancreatic tumor tissues, expression of spindle checkpoint genes was significantly up-regulated (center, in red) as compared to their normal counterparts. Up-regulation of the expression of spindle checkpoint genes will result in the suppression of the CDC20 activity that regulates anaphase promoting complex (APC/C) activity. The dotted blue arrows indicate a correlation of the expression in both lung carcinomas and pancreatic carcinomas.*

out with pancreatic carcinomas and lung carcinomas. Genes whose expression differed between tumor and corresponding normal tissues were ranked by T-values determined from the true Fisher's ratios and background Fisher's ratios, calculated from various combinations of the tumor and normal tissues. Validation by Welch's *t*-test revealed that differences between tumor and normal tissues in the expression of the top 150 genes ranked by T-values were considered to be statistically significant, because *p*-values were below 0.05. Performance of this screening procedure was reasonably high, because cluster analysis with the genes ranked top 150 in each tumor type clearly distinguish tumor from normal specimens. Genes ranked in the top 150 include many genes responsible for G2-M transition, especially for mitotic spindle assembly and chromosome segregation, strongly suggesting that one of the most remarkable features of tumor cells *in vivo* is the altered expression of genes involved in G2-M transition. In fact, cluster analysis with genes involved in mitotic spindle assembly and chromosome segregation also clearly distinguish tumor tissues from normal tissues in both lung and pancreas specimens.

Among the genes whose expression was significantly different in the tumor tissues as compared to their normal counterparts, 11 genes were commonly identified in two different tumor types with different tissue types and stages. Furthermore, 9 out of the 11 genes were found to be responsible for mitotic spindle assembly or chromosome segregation at the metaphase to anaphase transition, and the expression of all 9 genes were up-regulated in tumor cells as compared to their normal counterpart. Among these genes, *MAD2L1, BUB1, BUB1B, HEC* and *CENPE* encode spindle checkpoint proteins that are responsible for monitoring the attachment of microtubules to kinetochore. Furthermore, the expressions of other cell cycle and kinetochore-related genes such as *ZWINT, KNSL1, SMC4L1* and *CCNB1* also increased in both lung carcinomas and pancreatic carcinomas. *ZWINT* was originally identified as a gene for a protein that interacts with *ZW10*, whose defect caused aneuploidity in *Drosophila* and was shown to regulate anaphase onset in a tension-sensitive manner (24). *KNSL1* and *SMC4L1* encode a microtubule protein necessary for

mitotic spindle formation and a protein essential for mitotic chromosome condensation, respectively (25). The reason for the increased expression of the G2-M checkpoint genes in tumor tissues remains unknown, but the sensitivity and specificity of tumors to M-phase inhibitors such as taxanes, vinorelbine and epothilones may be attributable to an increased expression of G2-M checkpoint genes in tumor cells.

We applied Pearson's correlation in order to explore the expression network of spindle checkpoint genes. A search for genes whose expression correlated with that of *MAD2L1, BUB1, BUB1B, HEC,* or *CENPE* yielded 40 genes. Among these 40, 13 genes including *YES1* (26, 27), *CCNB1* (28, 29), *TOP2A* (and truncated form of topoisomerase) (30-32), *TOPBP1* (33), *STK15/Aurola A* (34), *TTK* (35), *Hsp90* (36) and alpha centractin (37) are involved in the metaphase to anaphase transition. The predicted gene expression network is summarized in Figure 6. The genes identified by the correlation analysis have not been reported as spindle checkpoint genes; however, several lines of evidence suggest that they are involved in kinetochore and/or spindle function. Both kinesin-related protein and alpha-centractin are thought to be responsible for kinetochore movement (37). CENPF shares a sequence homology with kinesins and localizes at the kinetochore plate to regulate kinetochore maturation (38). In addition, CENPF interacts with the CENPE (13), and CENPE also interacts with BUB1B (39). TTK, STK15 and YES all possess kinase activities and affect chromosome segregation. TTK, a human homologue of yeast MPS1, is required for the assembly of spindle checkpoint proteins (35). STK15/Aurora A kinase has been shown to be essential for chromosome segregation and centrosome functions (34). Furthermore, over-expression of STK15 in mammalian cells resulted in aneuploidy (34). YES, an src-related protein tyrosine kinase, is likely to be involved in mitotic progression because an inhibitor of this kinase interfered with spindle assembly (26, 27). HSP90 is a core centrosomal component and treatment of the cells with its specific inhibitor, geldanamycin, caused aberrant mitotic spindles (36). In *Drosophila*, the Cdc37/Hsp90 complex modulates a function of Aurora B kinase that is essential for chromosome segregation (40). TOP2A codes for topoisomerase that is necessary for the maintenance and segregation of the mitotic chromosomes (30, 32). Finally, CCNB is a cyclin responsible for the metaphase to anaphase transition (29). Thus, correlation analysis is a useful method to explore the functional networks of genes with mRNA expression profiles.

Acknowledgements

We thank F. Ford for proofreading the manuscript.

References

1 Ginsberg RJ, Vokes EE and Raben A: Non-small cell lung cancer. *In*: Cancer, Principles and Practice or Oncology (Devita VT Jr, Hellman S and Rosenberg SA, ed.), 5th edition, Lippincott-Raven, NewYork, pp. 858-911, 1997.

2 Evans DB, Abbruzzese JL and Rcih TA: Cancer of pancreas. *In*: Cancer, Principles and Practice or Oncology (Devita VT Jr, Hellman S and Rosenberg SA, ed.), 5th edition, Lippincott-Raven, NewYork, pp. 1054-1087, 1997.

3 Mohr S, Leikauf GD, Keith G and Rihn BH: Microarrays as cancer keys: an array of possibilities. J Clin Oncol *20*: 3165-75, 2002.

4 Guo QM: DNA microarray and cancer. Curr Opin Oncol *15*: 36-43, 2003.

5 Iizuka N, Oka M, Yamada-Okabe H, Mori N, Tamesa T, Okada T, Takemoto N, Tangoku A, Hamada K, Nakayama H, Miyamoto T, Uchimura S and Hamamoto Y: Comparison of gene expression profiles between hepatitis B virus- and hepatitis C virus-infected hepatocellular carcinoma by oligonucleotide microarray data on the basis of a supervised learning method. Cancer Res *62*: 3939-3944, 2002.

6 Iizuka N, Oka M, Yamada-Okabe H, Nishida M, Maeda Y, Mori N, Takao T, Tamesa T, Tangoku A, Tabuchi H, Hamada K, Nakayama H, Ishitsuka H, Miyamoto T, Hirabayashi A, Uchimura S and Hamamoto Y: Oligonucleotide microarray for prediction of early intrahepatic recurrence of hepatocellular carcinoma after curative resection. Lancet *361*: 923-929, 2003.

7 Eisen MB, Spellman PT, Brown PO and Botstein D: Cluster analysis and display of genome-wide expression patterns. Proc Natl Acad Sci USA *95*: 14863-14868, 1998.

8 Risinger JI, Umar A, Barrett JC and Kunkel TA: A hPMS2 mutant cell line is defective in strand-specific mismatch repair. J Biol Chem *270*: 18183-18186, 1995.

9 Guarne A, Junop MS and Yang W: Structure and function of the N-terminal 40 kDa fragment of human PMS2: a monomeric GHL ATPase. EMBO J *20*: 5521-5531, 2001.

10 Warren CD, Brady DM, Johnston RC, Hanna JS, Hardwick KG and Spencer FA: Distinct chromosome segregation roles for spindle checkpoint proteins. Mol Boil Cell *13*: 3029-3041, 2002.

11 Fang G: Checkpoint protein BubR1 acts synergistically with Mad2 to inhibit anaphase-promoting complex. Mol Biol Cell *13*: 755-766, 2002.

12 Chen RH: BubR1 is essential for kinetochore localization of other spindle checkpoint proteins and its phosphorylation requires Mad1. J Cell Biol *158*: 487-496, 2002.

13 Abrieu A, Kahana JA, Wood KW and Cleveland DW: CENP-E as an essential component of the mitotic checkpoint *in vitro*. Cell *102*: 817-826, 2000.

14 Martin-Lluesma S, Stucke VM and Nigg EA: Role of HEC1 in spindle checkpoint signaling and kinetochore recruitment of Mad1/Mad2. Science *297*: 2267-2270, 2002.

15 Gorbsky GJ, Chen RH and Murray AW: Microinjection of antibody to Mad2 protein into mammalian cells in mitosis induces premature anaphase. J Cell Biol *141*: 1193-1205, 1998.

16 Shah JV and Cleveland DW: Waiting for anaphase: Mad2 and the spindle assembly checkpoint. Cell *103*: 997-1000, 2000.

17 Zhang Y and Lees E: Identification of an overlapping binding domain on Cdc20 for Mad2 and anaphase-promoting complex: model for spindle checkpoint regulation. Mol Cell Biol *21*: 5190-5199, 2001.

18 Skoufias DA, Andreassen PR, Lacroix FB, Wilson L and Margolis RL: Mammalian mad2 and bub1/bubR1 recognize distinct spindle-attachment and kinetochore-tension checkpoints. Proc Natl Acad Sci USA *98*: 4492-4497, 2001.

19 Yu H: Regulation of APC-Cdc20 by the spindle checkpoint. Curr Opin Cell Biol *14*: 706-714, 2002.

20 Cleveland DW, Mao Y and Sullivan KF: Centromeres and kinetochores: from epigenetics to mitotic checkpoint signaling. Cell *112*: 407-421, 2003.

21 Musacchio A and Hardwick KG: The spindle checkpoint: structural insights into dynamic signaling. Nat Rev Mol Cell Biol *3*: 731-741, 2002.

22 Crnogorac-Jurcevic T, Efthimiou E, Nielsen T, Loader J, Terris B, Gordon S, Baron A, Scarpa A and Lemoine NR: Expression profiling of microdissected pancreatic adenocarcinomas. Oncogene *21*: 4587-4594, 2002.

23 Nakamura T, Furukawa Y, Nakagawa H, Tsunoda T, Ohigashi H, Murata K, Ishikawa O, Ohgaki K, Kashimura N, Miyamoto M, Hirano S, Kondo S, Katoh H, Nakamura Y and Katagiri T: Genome-wide cDNA microarray analysis of gene expression profiles in epithelial cells selected for purity by laser microdissection. Oncogene *23*: 1-16, 2004.

24 Starr DA, Saffery R, Li Z, Simpson AE, Choo KH, Yen TJ and Goldberg ML: HZwint-1, a novel human kinetochore component that interacts with HZW10. J Cell Sci *113*: 1939-1950, 2000.

25 Hirano T: The ABCs of SMC proteins: two-armed ATPase for chromosome condensation, cohesion, and repair. Genes Develop *16*: 399-414, 2002.

26 Roche S, Fumagalli S and Courtneidge SA: Requirement for Src family protein tyrosine kinases in G2 for fibroblast cell division. Science *269*: 1567-1569, 1995.

27 Moasser MM, Srethapakdi M, Sachar KS, Kraker AJ and Rosen N: Inhibition of Src kinases by a selective tyrosine kinase inhibitor causes mitotic arrest. Cancer Res *59*: 6145-652, 1999.

28 Chang CD, Xu N, Kathy Q and Luo KQ: Degradation of Cyclin B is required for the onset of anaphase in mammalian cells. J Biol Chem *278*: 37865-37873, 2003.

29 Wang Q, Moyret-Lalle C, Couzon F, Surbiguet-Clippe C, Saurin J-C, Lorca T, Navarro C and Puisieux A: Alterations of anaphase-promoting complex genes in human colon cancer cells. Oncogene *22*: 1486-1490, 2003.

30 Tavormina PA, Come MG, Hudson JR, Mo YY, Beck WT and Gorbsky GJ: Rapid exchange of mammalian topoisomerase II alpha at kinetochores and chromosome arms in mitosis. J Cell Biol *158*: 23-29, 2002.

31 Null AP, Hudson J and Gorbsky GJ: Both alpha and beta isoforms of mammalian DNA topoisomerase II associate with chromosomes in mitosis. Cell Growth Differ *13*: 325-333, 2002.

32 Kallio M and Lahdetie J: Effects of the DNA topoisomerase II inhibitor merbarone in male mouse meiotic divisions *in vivo*: cell cycle arrest and induction of aneuploidy. Environ Mol Mutagen *29*: 16-27, 1997.

33 Yamamoto R R, Axton JM, Yamamoto Y, Saunders RD, Glover DM and Henderson DS: The *Drosophila* mus101 gene, which links DNA repair, replication and condensation of heterochromatin in mitosis, encodes a protein with seven BRCA1 C-terminus domains. Genetics *156*: 711-721, 2000.

34 Anand S, Penrhyn-Lowe S and Venkitaraman AR: AURORA-A amplification overrides the mitotic spindle assembly checkpoint, inducing resistance to Taxol. Cancer Cell *3*: 51-62, 2003.

35 Stucke VM, Sillje HHW, Arnaud L and Nigg EA: Human Mps1 kinase is required for the spindle assembly checkpoint but not for centrosome duplication. EMBO J *21*: 1723-1732, 2002.

36 Clark IB and Meyer DI: Overexpression of normal and mutant Arp1 alpha (centractin) differentially affects microtuble organization during mitosis and interphase. J Cell Science *112*: 3507-3518, 1999.

37 Lange BMH, Rebollo E, Herold A and Gonzalez C: Cdc37 is essential for chromosome segregation and cytokinesis in higher eukaryotes. EMBO J *21*: 5364-5374, 2002.

38 Choo AKH: Centromere proteins of higher eukaryotes. *In*: The Centromere (Choo AKH, ed.). Oxford University Press (NewYork, N.Y.) pp.144-253.

39 Chan GKT, Schaar BT and Yen TJ: Characterization of the kinetochore binding domain of CENP-E reveals interaction with the kinetochore proteins CENP-F and hBUBR1. J Cell Biol *143*: 49-63, 1998.

40 Lange BMH, Bachi A, Wilm M and Gonzalez C: Hsp90 is a core centrosomal component and is required at different stages of the centrosome cycle in *Drosophila* and vertebrates. EMBO J *19*: 1252-1262, 2000.

Received May 19, 2004
Accepted June 3, 2004